

IDEAL MHD STABILITY OF FLUX-CORE SPHEROMAKS

F. Alladio, P. Micozzi and F. Rogier¹

CR-ENEA, CP 65, 00044 Frascati (Rome), Italy - ¹ONERA de Toulouse, France

1. INTRODUCTION

Chandrasekhar-Kendall-Furth (CKF) configurations [1] are a novel approach to magnetic confinement. They contain a magnetic separatrix, which divides a "main spherical torus" (with winding number, inverse of the rotational transform, $q=1/\iota$, $q_0^{ST} \sim 1.0$ on axis and $q_{95}^{ST} \sim 2.0$ at the separatrix), two "secondary tori" on top and bottom and an elongated "spheromak" discharge (such that $q_0^P \sim 3$ on the symmetry axis, $q_{95}^P \sim 5$ at the separatrix) surrounding the three tori. Unrelaxed ($\nabla p \neq 0$) CKF configurations can be stable to all low- n ideal MHD modes, up to unity beta values, $\beta = 2\mu_0 \langle p \rangle_{vol} / \langle B^2 \rangle_{vol} = 1$. The PROTO-SPHERA experiment (see Fig. 1) will study the properties of a CKF configuration where a Hydrogen force-free screw pinch, fed by electrodes, replaces in part the surrounding spheromak discharge, while "divertor" poloidal field coils replace the secondary tori. PROTO-SPHERA, with a longitudinal pinch current $I_e = 60$ kA, will produce a spherical torus of diameter $2 \cdot R_{sph} = 70$ cm, aspect ratio $A = 1.2 \div 1.3$, carrying a toroidal current $I_p = 120 \div 240$ kA.

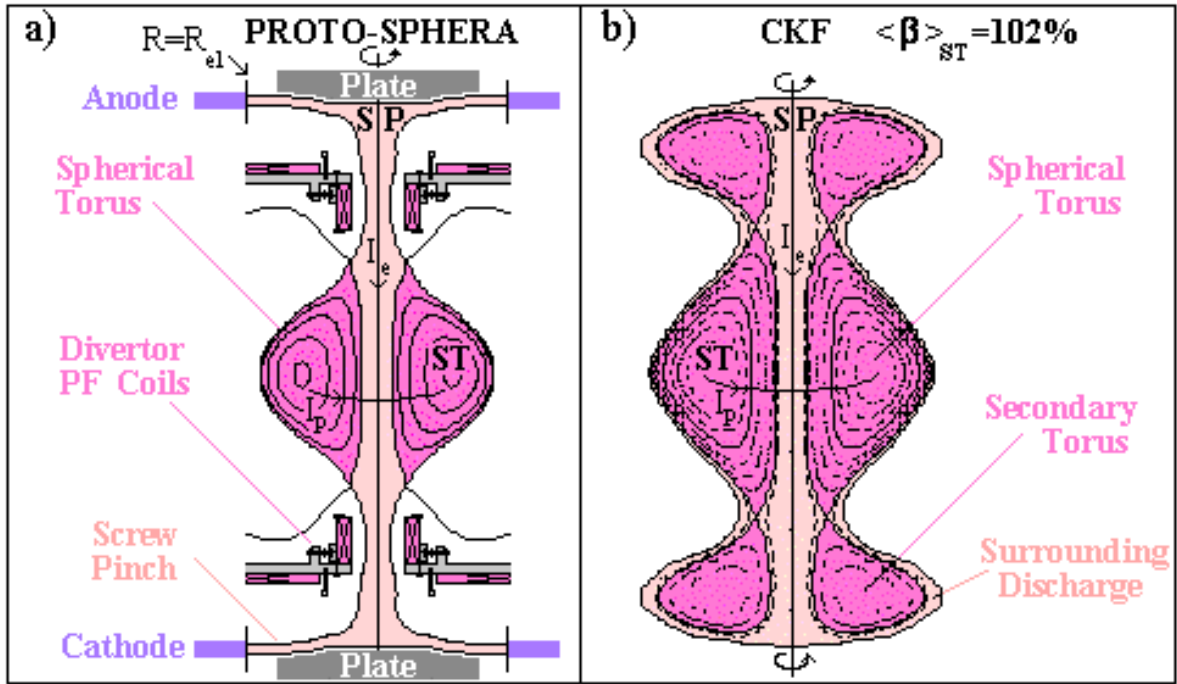


Fig. 1. Comparison between: a) PROTO-SPHERA and b) an unrelaxed CKF configuration.

In PROTO-SPHERA resistive MHD instabilities are required to inject magnetic helicity from the screw pinch into the spherical torus, but the combined equilibrium should be stable in ideal MHD. New ideal MHD stability codes have been written to analyze PROTO-SPHERA.

2. BOOZER COORDINATES ON OPEN FIELD LINES

The Boozer coordinates [2] (ψ_T -radial=toroidal flux/ 2π in tori, θ -poloidal, ϕ -toroidal) simplify the expression of the ideal MHD stability problem [3]. $I(\psi_T) = \mu_0 I_p / 2\pi$ and $f(\psi_T) = RB_\phi = \mu_0 I_{dia} / 2\pi$ are the normalized toroidal and poloidal currents; $\sqrt{g} = [f(\psi_T) + \iota(\psi_T)I(\psi_T)] / B^2$ is the

Jacobian. The nonorthogonality of the Boozer coordinates is expressed by the two terms: $\gamma_*(\psi_T, \theta) = \bar{\nabla}\psi_T \cdot (\bar{\nabla}\theta - \iota\bar{\nabla}\phi) / |\bar{\nabla}\psi_T|^2$ and $\beta_* = \beta_*(\psi_T, \theta)$, from the covariant field representation $\bar{\mathbf{B}} = \beta_*\bar{\nabla}\psi_T + \iota\bar{\nabla}\theta + f\bar{\nabla}\phi$. The combined PROTO-SPHERA equilibrium is analyzed in term of the poloidal flux function $\psi = 2\pi R A_\phi$. The open field lines in the screw pinch (SP) span the range $(0 < \psi < \psi_X)$, the closed field lines inside the spherical torus (ST) the range $(\psi_X < \psi < \psi_{\max})$. The length parameter $s(\psi)$ on the SP open field lines is: $s=0$ on the lower electrode, $s=s_{\text{eq}}(\psi)$ on the equator and $s=s_0(\psi)$ where the poloidal Boozer angle is $\theta=0$.

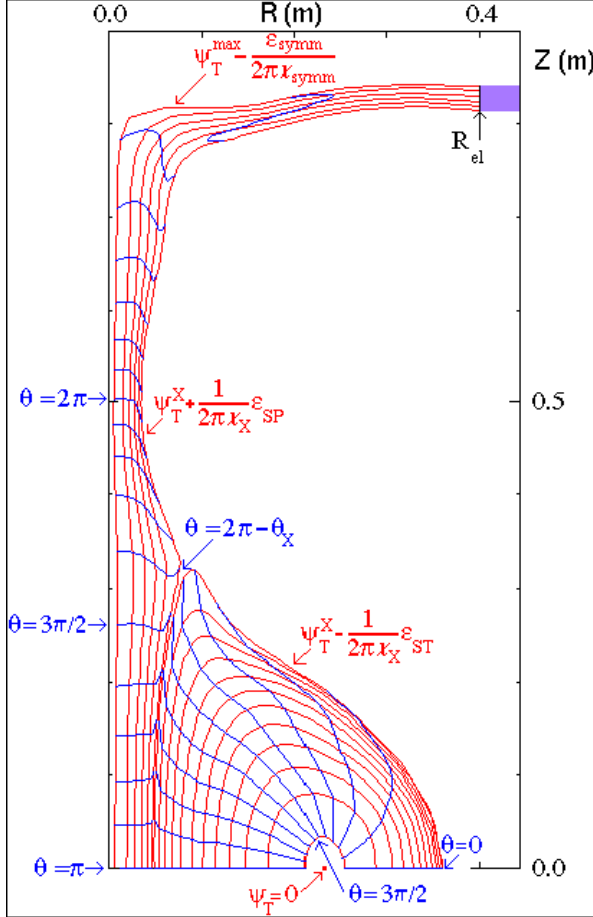


Fig. 2. Boozer coordinates for PROTO-SPHERA

Boozer coordinates into the SP (Fig. 2) are fixed by conditions at the ST-SP interface ($\psi = \psi_X$):

- 1) Continuity of $\bar{\nabla}\psi_T$, θ and ϕ .
- 2) Contiguity of field lines $\theta_0 = \theta - \iota(\psi)\phi$.
- 3) Continuity of $\iota(\psi) = \iota_X$.
- 4) Continuity of $I(\psi) = I_X$.

Line integral definitions are then provided inside

the SP, for:
$$I(\psi) = \frac{1}{\pi} \int_{s_0(\psi)}^{s_{\text{eq}}(\psi)} \mathbf{B}_p \hat{\mathbf{e}}_p \cdot d\bar{\mathbf{l}}_p,$$

$$\iota(\psi) = \frac{\pi}{f(\psi) \int_{s_0(\psi)}^{s_{\text{eq}}(\psi)} \frac{1}{R^2 B_p} \hat{\mathbf{e}}_p \cdot d\bar{\mathbf{l}}_p}.$$
 On the ST side ι_X

is calculated at $\psi = \psi_X + \epsilon_{\text{ST}}$, with $\epsilon_{\text{ST}} \sim 10^{-3} |\psi_{\max} - \psi_X|$, on the SP side $\iota = \iota_X$ at $\psi = \psi_X - \epsilon_{\text{SP}}$, with $\epsilon_{\text{SP}} \neq \epsilon_{\text{ST}}$. Given I_X and ι_X , θ is evaluated on the ST-SP interface, yielding $s = s_0(\psi_X - \epsilon_{\text{SP}})$. For all the flux surfaces in the range $(0 < \psi < \psi_X - \epsilon_{\text{SP}})$, $s_0(\psi)$ is calculated from the force-free equilibrium condition: $df/d\psi + \iota dI/d\psi = 0$. It provides a first order integro-differential equation for $s_0(\psi)$, solved iteratively, with boundary condition $s_0(\psi_X - \epsilon_{\text{SP}})$. Knowledge of $s_0(\psi)$ allows to calculate $I(\psi)$, $\iota(\psi)$ and then (ψ_T, θ, ϕ) all over the pinch.

3. THE IDEAL MHD STABILITY CODES STABLE AND STABLEC

The compressible perturbed displacement $\bar{\xi}$ is expressed in Boozer coordinates, in terms of normal $\xi^\psi = \bar{\xi} \cdot \bar{\nabla}\psi_T$, binormal $\eta = \bar{\xi} \cdot (\bar{\nabla}\theta - \iota\bar{\nabla}\phi)$ and parallel $\mu = -\sqrt{g} \bar{\xi} \cdot \bar{\nabla}\phi$ components, which are expanded in Fourier series: $\xi^\psi = \sum_i \xi_i(\psi_T) \sin(m_i\theta - n\phi)$, $\eta = \sum_i \eta_i(\psi_T) \cos(m_i\theta - n\phi)$, $\mu = \sum_i \mu_i(\psi_T) \cos(m_i\theta - n\phi)$. The perturbed kinetic energy is a quadratic form of (ξ_i, η_i, μ_i) . The perturbed potential magnetic energy is a quadratic form of $(\xi_i, \eta_i, \mu_i, \partial \bar{\xi}_i / \partial \psi_T)$. Two even-spaced meshes are set up: inside the ST, $\psi_T^i = i \Delta\psi_T^{\text{ST}}$, for $i=0, \dots, N_\psi^{\text{ST}}$, with $N_\psi^{\text{ST}} \Delta\psi_T^{\text{ST}} = \psi_T^X - \epsilon_{\text{ST}} / 2\pi k_X$; inside the SP, $\psi_T^i = \psi_T^X + \epsilon_{\text{SP}} / 2\pi k_X + (i - N_\psi^{\text{ST}} - 1) \Delta\psi_T^{\text{SP}}$, for $i = N_\psi^{\text{ST}} + 1, \dots, N_\psi^{\text{ST}} + N_\psi^{\text{SP}}$, with $(N_\psi^{\text{SP}} - 1) \Delta\psi_T^{\text{SP}} = (\psi_T^{\max} - \psi_T^X) - \epsilon_{\text{SP}} / 2\pi k_X - \epsilon_{\text{symm}} / 2\pi k_{\text{symm}}$. At the ST-SP interface, ideal MHD forbids any discontinuity of the normal component ξ_i , whereas discontinuities of the tangential components (η_i, μ_i) are allowed for. The code STABLE solves the eigenvalue problem

$\vec{W} \cdot |\vec{x}\rangle = \omega^2 \vec{K} \cdot |\vec{x}\rangle$, where the total potential magnetic energy matrix \vec{W} and the (positive definite) kinetic energy matrix \vec{K} are symmetric and block-diagonal, $\vec{x} \equiv (\xi_l^i, \eta_l^i, \mu_l^i)$ is the eigenvector, and ω^2 the eigenvalue. However, as the PROTO-SPHERA plasma extends up to the symmetry axis $R=0$, the representation of the perturbed displacement used in the code STABLE,

$$\vec{\xi} = \xi^\psi \frac{\bar{\nabla}\psi_T}{|\bar{\nabla}\psi_T|^2} + (\eta - \gamma_* \xi^\psi) \frac{\vec{B} \wedge \bar{\nabla}\psi_T}{B^2} + \left(\frac{\beta_*}{B^2} \xi^\psi + \frac{I}{B^2} \eta - \mu \right) \vec{B},$$

- 1) $\bar{\nabla}\psi_T$ goes to zero like $|\bar{\nabla}\psi_T| \approx R$, therefore the regularity condition $\xi^\psi(\psi_T^{\max})=0$ should be imposed at the symmetry axis. However, along the plasma disks, on top and bottom of the configuration, the flux surface $\psi_T = \psi_T^{\max}$ branches from the symmetry axis (see Fig. 1.a and Fig. 2), with $\bar{\nabla}\psi_T \neq 0$. Therefore no regularity condition on $\xi^\psi(\psi_T^{\max})$ should be imposed on the plasma disks, unless upper and lower stabilizing conducting plates are inserted (Fig. 1a).
- 2) At the degenerate X-points ($B=0$) on $R=0$ the prescription that $\eta(\psi_T \rightarrow \psi_T^{\max}) \sim O(r^{1/2+\epsilon})$ must hold. So the regularity condition $\eta(\psi_T^{\max})=0$ should be imposed, but this cannot be done, as the derivative $\partial\eta\partial\psi_T$ of the binormal displacement does not appear in the energy principle.

The only proper way of treating the flux surface $\psi_T = \psi_T^{\max}$ is to change two of the displacement components to $\tilde{\xi} = \xi^\psi / |\bar{\nabla}\psi_T|$ and $\tilde{\eta} = \eta/B$; with these new variables no regularity conditions have to be imposed at the symmetry axis. The code STABLEC is completely analogous to the code STABLE, but works in terms of the components $(\tilde{\xi}, \tilde{\eta}, \mu)$ of the perturbed displacement:

$$\vec{\xi} = \tilde{\xi} \frac{\bar{\nabla}\psi_T}{|\bar{\nabla}\psi_T|} + \left(\tilde{\eta} - \gamma_* \frac{|\bar{\nabla}\psi_T|}{B} \tilde{\xi} \right) \frac{\vec{B} \wedge \bar{\nabla}\psi_T}{B} + \left(\beta_* \frac{|\bar{\nabla}\psi_T|}{B} \tilde{\xi} + \frac{I}{B} \tilde{\eta} - \mu \right) \vec{B}.$$

however two disadvantages: the expression of the perturbed potential energy is more complicated and the convergence of ω^2 requires a more extended range of the poloidal numbers m_l . Both codes have been validated on the well-known stability results [4] of the analytic Solov'ev's equilibria.

4. VACUUM MAGNETIC ENERGY WITH MULTIPLE PLASMA BOUNDARIES

The treatment of the vacuum magnetic energy contribution in PROTO-SPHERA is complicated by the presence of three plasma-vacuum surfaces (see Fig. 2):

$$\begin{aligned} \psi_T^{v1} &= \psi_T^X - \varepsilon_{ST}/2\pi l_X \quad (i=N_\psi^{ST}), & \text{with rotational transform } t^{v1} &= t_X; \\ \psi_T^{v2} &= \psi_T^X + \varepsilon_{SP}/2\pi l_X \quad (i=N_\psi^{ST}+1), & \text{with rotational transform } t^{v2} &= t_X; \\ \psi_T^{v3} &= \psi_T^{\max} - \varepsilon_{\text{symm}}/2\pi l_{\text{symm}} \quad (i=N_\psi^{ST} + N_\psi^{SP}), & \text{with rotational transform } t^{v3} &= t_{\text{symm}}. \end{aligned}$$

In general, couplings in the matrix elements among all the three surfaces can exist. The vacuum energy of the magnetic surface ψ_T^{v3} is however decoupled from the other two surfaces by the closed conducting path of the screw pinch current I_e , which flows into the electrodes. The other two surfaces ψ_T^{v1} and ψ_T^{v2} are very near, have been chosen in such a way as to have the same rotational transform t_X and furthermore the continuity condition imposes $\xi_l(\psi_T^{v1}) = \xi_l(\psi_T^{v2})$. These choices simplify the coupling between the vacuum energy of ψ_T^{v1} and ψ_T^{v2} . The vacuum perturbed scalar potential is solved, by a 2D finite element method that can fit any shape of the plasma and of the surrounding axisymmetric conducting walls (vacuum vessel and PF coil cases).

5. IDEAL MHD STABILITY OF TS-3 AND OF PROTO-SPHERA

To test the stability codes upon an experiment, the equilibria of the TS-3 flux-core-spheromak experiment [5] have been simulated (Fig. 3). TS-3 did not have plasma disks inside separate electrode chambers, but a simple straight pinch fed by cylindrical electrodes inside the vessel,

which acted as the only surrounding axisymmetric conducting wall. The codes STABLEC and STABLE, with $\xi^\psi(\psi_T^{\max})=0$, calculate the same ideal MHD stability results. In agreement with the experiment, they confirm that TS-3, with $I_e=40$ kA, was limited to $I_p \leq 50$ kA and to $A \geq 1.6$.

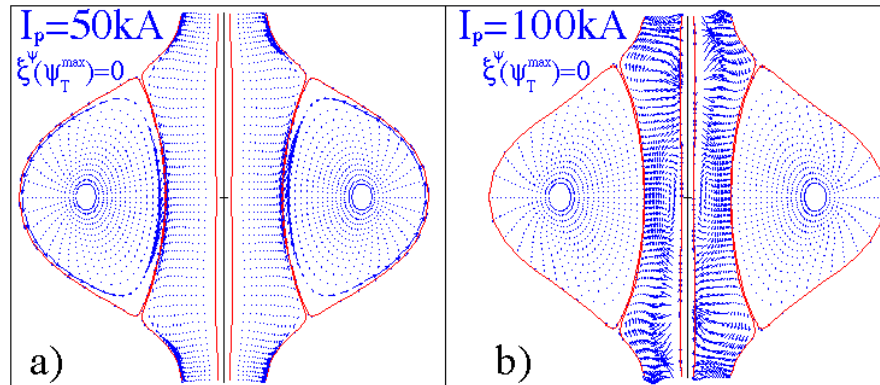


Fig. 3. Displacement plot for TS-3 with $I_e=40$ kA: a) stable motion at $I_p=50$ kA, b) global instability at $I_p=100$ kA.

For the equilibria of PROTO-SPHERA, accounting all conducting walls, STABLEC calculates a stability limit to the ratio between the toroidal ST current I_p and the longitudinal SP current I_e .

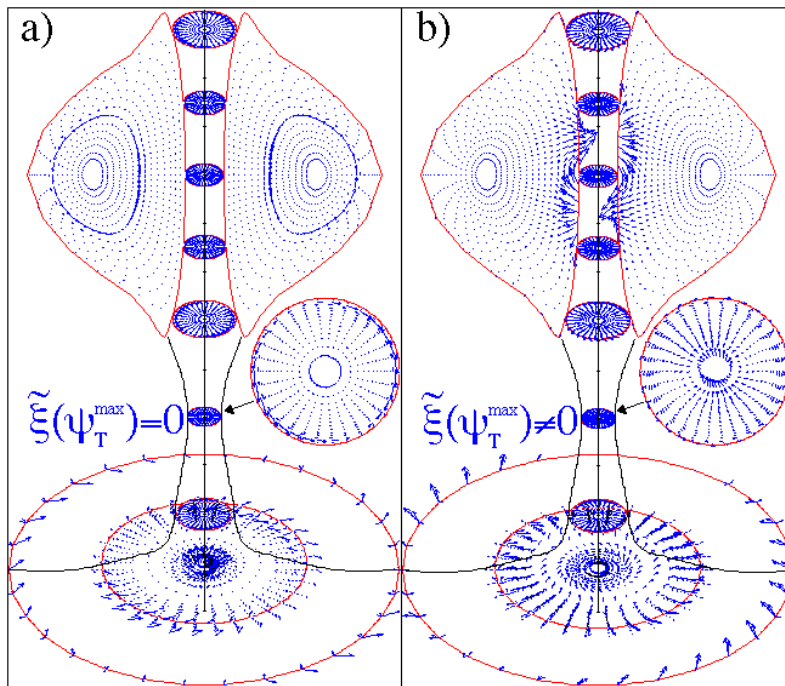


Fig. 4. Displacement plot for PROTO-SPHERA with $I_e=40$ kA, $I_p=180$ kA, $\beta_{ST} \sim 20\%$: a) stable motion if $\tilde{\xi}(\psi_T^{\max})=0$; b) global instability if $\tilde{\xi}(\psi_T^{\max}) \neq 0$.

The upper I_p/I_e limit depends upon the ST beta value $\beta_{ST}=2\mu_0 \langle p \rangle_{ST} / \langle B^2 \rangle_{ST}$.

The ratio I_p/I_e can be increased if the upper and lower stabilizing conducting plates (Fig. 1a) are inserted (Fig. 4).

At $\beta_{ST} \sim 30\%$ the ideal MHD stability calculated by STABLEC sets the limit to $I_p=I_e$, at a ST aspect ratio $A=1.3$.

At $\beta_{ST} \sim 20\%$ I_p can reach $2 \cdot I_e$ at $A=1.3$, or, with stabilizing plates, $3 \cdot I_e$ at $A=1.25$.

At $\beta_{ST} \sim 10\%$ I_p can reach $2 \cdot I_e$ at $A=1.3$, or, with stabilizing plates, $4 \cdot I_e$ at $A=1.2$ (the design limit of PROTO-SPHERA).

- [1] P. Micozzi et al., *CKF Configurations for Magnetic Confinement*, this Workshop
- [2] Boozer A. H., *Phys. Fluids* **24** (1981) 1999
- [3] Cooper W.A., *Plasma Phys. Contr. Fusion* **34** (1992) 1011
- [4] Chance M.S. et al., *J. of Comput. Phys.* **28** (1978) 1
- [5] Amemiya N., Morita A. and Katsurai M., *J. Phys. Soc. Jpn.* **63** (1993) 1552